Available online at www.sciencedirect.com

SCIENCE DIRECT®

Vision Research 44 (2004) 9–18

Vision Research

www.elsevier.com/locate/visres

The relationship between full field electroretinogram and perimetry-like visual thresholds in RCS rats during photoreceptor degeneration and rescue by cell transplants

Y. Sauvé *, B. Lu, R.D. Lund

Moran Eye Center, Ophthalmology and Visual Sciences, University of Utah, Health Sciences Center, 50 North Medical Drive, Salt Lake City, UT 84132, USA

Received 22 April 2003; received in revised form 10 June 2003

Abstract

Dark-adapted full field electroretinogram (ERG) and visual receptive field thresholds (recorded from the superior colliculus) were correlated in a model of retinal degeneration, the Royal College of Surgeons rat. In both untreated and retinal pigment epithelium cell transplanted rats, optimal correlation was between *b*-wave amplitude and preserved visual field area with thresholds under a defined level.

The work shows that the magnitude of the *b*-wave can be used to predict the computed area and degree of visual field preservation recorded in the central nervous system. These observations validate using ERG to assess residual visual function and the effect of transplantation.

Keywords: Retinal degeneration; Superior colliculus; Visual field perimetry; ERG; Transplantation

1. Introduction

Retinitis pigmentosa (RP) and age-related macular degeneration represent the main causes of blindness, worldwide, for which there is presently no effective treatment (for recent reviews see la Cour, Kiilgaard, & Nissen, 2002; Rivolta, Sharon, DeAngelis, & Dryja, 2002). Experimental animal models are being used to understand the disease process and formulate therapeutic strategies (for a recent review see Chader, 2002). Among these models, the Royal College of Surgeons (RCS) rat has been one of the most extensively characterized following the original studies by Bourne, Campbell, and Tansley (1938) and Dowling and Sidman (1962). A critical aspect in such experimental studies is the need to use functional assessments of vision that have relevant analogies with clinical diagnostics.

The standard clinical assessments of retinal function include the electroretinogram (ERG) to full field stimulation and static visual field perimetry. Despite the numerous studies on how ERG can predict the level of vision, its relationship with perimetry remains unclear. Several studies have pointed to the poor correlation between ERG parameters and size of remaining visual field (Arden et al., 1983; Fahle, Steuhl, & Aulhorn, 1991; Massof et al., 1984), and there have been reports that patients with some level of visual function have flat ERGs (Sieving, 1999). Then again, other reports show strong correlations between ERG and field size (Birch, Herman, deFaller, Disbrow, & Birch, 1987; Iannaccone et al., 1995; Sandberg, Weigel-DiFranco, Rosner, & Berson, 1996; Yagasaki, Jacobson, Apathy, & Knighton, 1988).

The ERG has been studied in detail in rodents (for a review see Nusinowitz, Ridder, & Heckenlively, 2002) and uses virtually identical procedures to those employed in patients. In contrast, there is no possibility of using precision human perimetry testing regimens in rodents: rats cannot fixate a LED and press a button upon noticing a small spot in their peripheral visual field. However, analogous data can be collected by recording visual responses at specific sites in the superior colliculus (where over 95% of retinal ganglion cells send direct projections): relative visual thresholds can be

* Corresponding author. Tel.: +1-801-585-2475.
E-mail address: yves.sauve@hsc.utah.edu (Y. Sauvé).

0042-6989/$ - see front matter © 2003 Elsevier Ltd. All rights reserved.
doi:10.1016/j.visres.2003.08.015

measured across the visual field, thereby providing a reliable point-to-point assessment of retinal function. Using this approach, we are in a position to explore possible correlations between ERG parameters and retinal sensitivity across the visual field in rodents and here we have used the RCS rat, both unoperated and after cell transplantation to limit the progression of photoreceptor degeneration.

The dystrophic RCS rat undergoes progressive photoreceptor degeneration due to a primary defect in retinal pigment epithelium (RPE) cells (D'Cruz et al., 2000). In pigmented RCS rats, most photoreceptors are lost in the first three months of life (Eisenfeld, LaVail, & LaVail, 1984). Elevations in visual thresholds become apparent by one month of age; from then onward, thresholds progressively increase until a plateau is reached at 6–8 months (Sauvé, Girman, Wang, Lawrence, & Lund, 2001). By contrast, two photoreceptor-driven ERG parameters (the *a*-wave and *b*-wave) disappear very early in the progress of the disease—by 50 and 100 days respectively (Bush, Hawks, & Sieving, 1995). The uniform progress of anatomical and functional deterioration makes it possible to investigate the correlations being examined here. Preventive subretinal transplantation of healthy RPE cell lines, performed in rats younger than a month of age, can lead to a significant degree of visual field preservation, which persists for at least 8 months of age (Coffey et al., 2002; Lund et al., 2001a, 2001b; Sauvé, Girman, Wang, Keegan, & Lund, 2002). Sham injections also result in rescue although the area and degree of preservation is significantly smaller. Previous studies using corneal ERG recordings have provided indications of change following therapeutic intervention (Jiang & Hamasaki, 1994; Machida et al., 2001; Vollrath et al., 2001; Yamazaki et al., 2002), but without any systematic correlation with other parameters of vision, the interpretation of the changes are sometimes hard to make.

The purpose of this study was to examine the relationship between ERG and perimetry-like parameters achieved by recording multiunit responses in the SC during the course of photoreceptor degeneration and after using a therapeutic intervention, cell transplantation, to slow its progress. With this information, better indication can be given of the value of using ERG as a suitable tool in screening efficacy of transplantation as well as other similar therapeutic treatments.

2. Methods

2.1. Animals

To avoid complications associated with the poor vision of albinos, all the work has been done on pigmented rats, either dystrophics (RCS rdy^+ p^+, $n = 63$) or non-dystrophic congenics (RCS rdy^- p^+, $n = 16$). All animals used in this study were bred in a colony at the University of Utah, and maintained under a 12 h light dark cycle (light cycle mean illumination: 30 cd/m^2). They were housed and handled with the authorization and supervision of the Institutional Animal Care and Use Committee from the University of Utah. Every procedure conformed to the National Institute of Health guidelines.

2.2. Therapeutic intervention: subretinal transplantation of a human RPE cell line

Photoreceptor rescue was achieved in dystrophic RCS rats by injecting a suspension of immortalized human RPE cells subretinally by a trans-scleral approach, at 3 weeks of age prior to significant elevation in thresholds across their visual field (Sauvé et al., 2001). The cell line used was the spontaneously arising ARPE-19 line available from the ATCC (American Tissue Culture Collection; reference number: CRL-2302).

The transplantation procedure was as previously described (Lund et al., 2001a; Sauvé et al., 2002). Briefly, 36 recipient dystrophic RCS rats were anesthetized with xylazine–ketamine (1 mg/kg i.p. of the following mixture: 2.5 ml xylazine at 20 mg/ml, 5 ml ketamine at 100 mg/ml, and 0.5 ml distilled water). Eighteen rats received cells and another 18 had injections of medium alone. All injections were unilateral: the contralateral eye served as untreated control. Cultures of ARPE-19 cells were trypsinized, washed and delivered as a suspension (2×10^5 per injection) in 2l of Ham's F10 medium through a fine glass pipette (internal diameter 75–150 μm) into the eye through a small scleral incision (Sauvé et al., 2002). All animals were maintained on cyclosporine administered in the drinking water (210 mg/l; resulting blood concentration: 250–300 μg/l; Coffey et al., 2002) from 2 to 3 days prior transplantation until sacrifice (from 5 to 8 months).

2.3. ERG recordings

Following overnight dark adaptation, animals were prepared for ERG recording under dim red light. Under anesthesia with a mixture of ketamine (150 mg/kg i.p.) and xylazine (10 mg/kg i.p.), the head was secured with a stereotaxic head holder and the body temperature monitored through a rectal thermometer and maintained at 38 °C using a homeothermic blanket. Pupils were dilated using equal parts of topical phenylephrine (2.5%) and atropine (1%). A drop of 0.9% saline was applied on the cornea to prevent its dehydration and allow electrical contact with the recording electrode (gold wire loop). A 25-gauge needle inserted under the scalp, between the two eyes, served as the reference electrode. All animals were tested the day prior to re-

cording threshold responses in the SC (see below for time points). In the case of animals with transplants and sham injections, they were tested longitudinally at about 30 day intervals from P31 up to the time of recording threshold responses in the SC.

Amplification (at 1–1000 Hz bandpass, without notch filtering), stimulus presentation, and data acquisition were provided by the UTAS-3000 system from LKC Technologies (Gaithersburg, MD). Recordings consisted of single flash presentations (standard 10 μs duration), with 3–5 presentations to verify the reliability of responsiveness. For dark-adapted intensity responses, stimuli were presented at six increasing intensities in one log steps varying from −3.6 to 1.4 log cd s/m^2 in luminance. Photopic intensity responses (30 cd/m^2 background) ranged from −1.6 to 2.9 log cd s/m^2 (−1.6, −0.6, 0.4, 1.4, 2.4 and 2.9 log cd s/m^2). To diminish effects of bleaching, inter-stimuli-intervals (ISI) were increased as the stimulus luminance was elevated from 10 s at lowest stimulus intensity (−3.6 log cd s/m^2) up to 2 min at highest stimulus intensity (1.4 log cd s/m^2 for scotopic and 2.9 log cd s/m^2 for photopic conditions). The maximal *b*-wave amplitude was that obtained during the flash intensity series, regardless of the stimulus intensity. The true V_{max} from fitting the data with a Naka–Rushton curve was not used here. Because ERG responses were often erratic at higher luminance levels in dystrophic animals and showed tendencies for depressed responses around 0.4 and 1.4 log cd s/m^2 (see Fig. 4) this made such curve fitting an unreliable exercise.

Criterion amplitudes were established at 20 μV for *a*- and *b*-waves, and at 10 μV for scotopic threshold response (STR)-like responses. The amplitude of the *b*-wave was measured from the *a*-wave negative peak up to the *b*-wave positive apex, and not up to the peak of oscillations, which can exceed the *b*-wave apex (see Nusinowitz et al., 2002).

The ERG protocols used in this study were not designed to systematically harvest the RPE-related *c*-waves. In order to quantify *c*-wave responses effectively, up to 10–30 responses had to be averaged to give reliable smooth *c*-waves. To avoid bleaching at higher illuminations, ISI had to be as high as 2 min. With such a protocol, data collection would take up to an hour per intensity, per eye.

2.4. Mapping of visual thresholds

Sensitivity maps were obtained across the visual field by recording multi-unit activity at 76 equidistant sites encompassing the entire surface of the superior colliculus, as previously described (Sauvé et al., 2001). In brief, under urethane anesthesia (1.25 g/kg, i.p.), the body temperature was maintained at 38 °C, the head held by a nose bar, the test eye stabilized with three equidistant subconjunctival sutures attached to the fixation frame and the pupil fully dilated with topical phenylephrine (2.5%) and atropine (1%). A non-correcting contact lens protected the cornea from dehydration-induced clouding.

A translucent hemisphere was positioned in front of the test eye and illuminated at 0.02 cd/m^2 and following one-hour period of adaptation, multi-unit recordings were made from the superficial layers of the SC using glass-coated tungsten electrodes (resistance: 0.5 MΩ, bandpass: 500 Hz–5 kHz). The microelectrode penetrations were made along a rectilinear grid of 400 μm steps. At sites where a response to whole eye illumination was found, an attempt was made to define a discrete receptive field (RF) position for that unit. The visual field was systematically searched by moving a spot of light (3° in diameter with luminance of up to 4.5 log cd/m^2 higher than background) across the surface of the translucent hemisphere. Once a response could be elicited in this manner, the RF was located and its center defined. The RF was then illuminated with a flashing light positioned at its center (spot of 3° diameter with 1 s duration at 3 s intervals). Neutral density filters were added progressively (minimal steps of 0.1 log filters; unfiltered stimulus was 4.5 log illumination above background) to establish the minimum illumination required to elicit a response, which was taken as the relative visual threshold according to the above described background adaptation. Response onset required a minimum of one more spike per 5 ms bins than the highest bin within 100 ms prestimulus. Electrophysiological testing was performed in a blind manner, with animals from different groups interspersed.

Dystrophic RCS rats with transplants or sham injections were studied longitudinally using ERGs from age P31 and then sacrificed at the time of SC mapping, starting at P150, then P180 and finally P200–220; $n = 6$ per group per time point. Due to the invasive nature of threshold mapping across the SC, these experiments were terminal, and never recovery procedures. Therefore, each animal was studied at a single time point. In the case of untreated dystrophic RCS rats, 27 animals were used for terminal SC mapping at time points encompassing P21 up to P180. In addition, six congenic non-dystrophic RCS rats were used for ERG recordings along this period.

2.5. Statistics

Error values accompanying averages were expressed as standard errors of the mean (SEM). Comparisons between two groups were made using: (1) Student *t*-test when data followed normal distributions; and (2) Mann–Whitney *U*-test when data did not follow a normal distribution. The level of correlation between ERG parameters and visual field area was evaluated based on the coefficient of determination (r^2) calculated

using Pearson correlation coefficient. The probability level at which the Null Hypothesis was rejected is represented as the value "p"; statistical significance was set at $p < 0.05$.

3. Results

3.1. Dark-adapted full field ERG

The progressive deterioration in ERG responsiveness is illustrated in Fig. 1 as changes in *a*- and *b*-wave amplitudes with age (see Fig. 2 for representative examples of ERG traces). By the time of completion of visual system maturation, at age P21, all dark-adapted full field ERG parameters were comparable to those of non-dystrophic congenic RCS rats. A week later, signs of deterioration were already obvious: by P28, there were considerable reductions in *a*- and *b*-wave amplitudes (over 50% loss) and slight prolongations in their implicit time (not illustrated). Amplitudes decreased to criterion response levels by P51 for the *a*-wave and P80–100 for the *b*-wave. Oscillations tended to be associated with the presence of an *a*-wave and vanished by P51. The visually driven ERG component that persisted the longest, up to P180, consisted of a slow negative deflection reminiscent of the STR.

Subretinal transplantation had a sustained effect on several components of the ERG. The most significant effect was on preservation of the *b*-wave, which could be recorded for as much as 100 days longer than in untreated animals, i.e. P180–220 (Figs. 2(c) and 3(right panel)). In addition to its prolonged persistence following transplantation, the *b*-wave showed significantly higher amplitudes than in untreated dystrophic rats. This was already evident 10 days post-transplantation, i.e. by P33. Statistically significant difference relative to

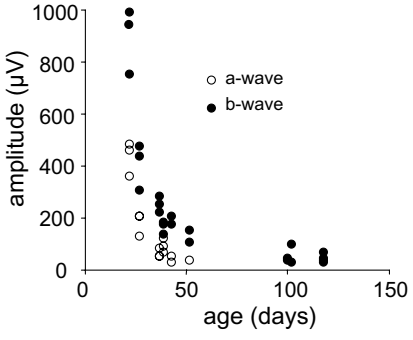

Fig. 1. Progressive loss of ERG responsiveness in untreated dystrophic RCS rats. The graph shows the maximal ERG *a*-wave (white circles) and *b*-wave (black circles) amplitude as a function of age. While values compare to that of non-dystrophic congenic RCS rats at 21 days, they rapidly fall within 30 days, approximating criterion amplitude (20 μV) by 50 and 100–120 days for *a*- and *b*-wave, respectively.

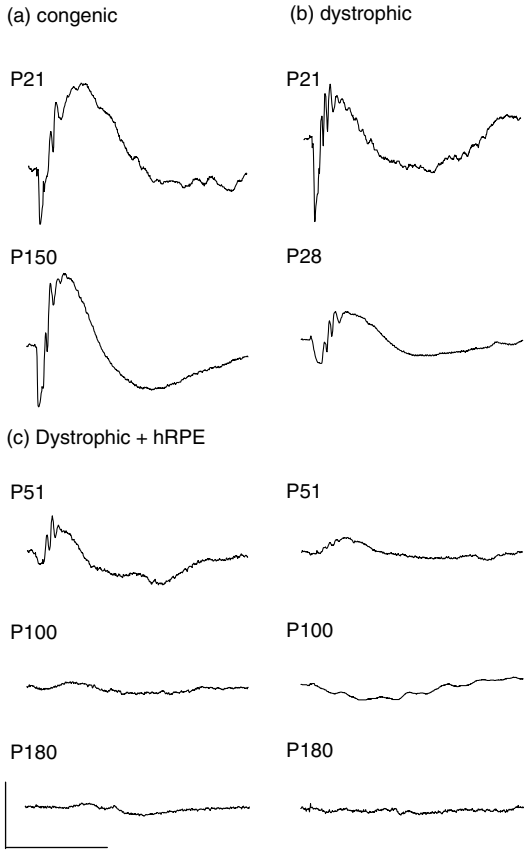

Fig. 2. Decline in ERG responsiveness during the course of retinal degeneration and the preventive effect of human cell lines. Examples were taken from ERG traces giving maximal *b*-wave amplitude during intensity response tests: in cases in which *b*-waves were no longer evident, traces show responses with maximal STR-like waves (see panel b at P100). Panels: (a) congenic at P21, P150 (upper left column); (b) untreated dystrophic RCS rats at P21, P28, P51, P100, P180 (right column); (c) dystrophic RCS rats with human cell line transplants, recorded at P51, P100, and P180 (lower left column). Scale bars: vertical = 500 μV; horizontal = 500 ms.

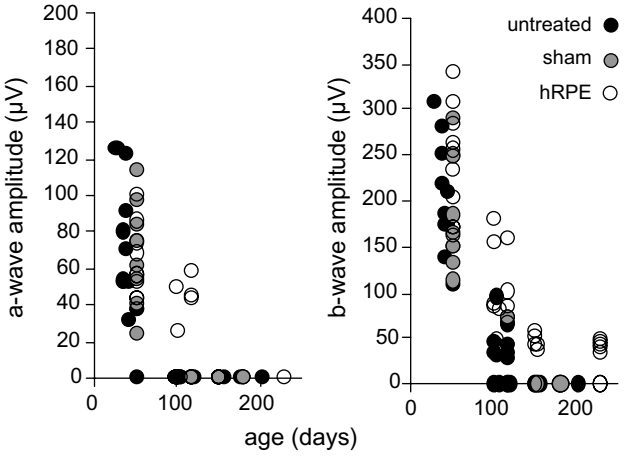

Fig. 3. Progressive loss of *a*- and *b*-wave amplitudes with age in dystrophic RCS rats and the preventive effect of transplantation. Ages presented start from P28. Left panel: *a*-wave; right panel: *b*-wave.

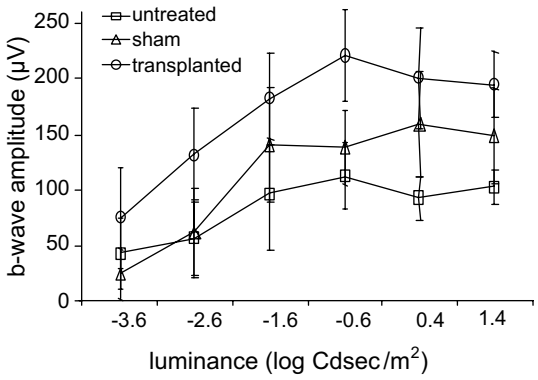

Fig. 4. Preservation of *b*-wave amplitude at P51, four weeks post-transplantation (circles) in comparison with untreated (squares) and sham-injected (triangles) eyes; $n = 8$ per group; error bars represent SEM. Statistical significance between transplant and sham-operated eyes was seen at -0.6 log cd s/m^2 ($p = 0.01$).

shams was attained by P51, i.e. 28 days post-operatively; Fig. 4 shows *b*-wave amplitudes from intensity response tests for various groups at P51. In addition to the transplant effects, sham operation also led to preservation of *b*-waves. This sham-related effect tended to be weaker and more variable, which might explain the absence of statistically significant differences between data from sham-operated and untreated eyes.

Transplantation also preserved *a*-wave responses although less consistently so (Fig. 3(left panel)). There was a significant preservation of the *a*-wave amplitude at P51, when transplanted eyes were compared with untreated eyes, but sham operations were equally successful in preserving the *a*-wave at this time point. Statistical difference between transplanted and sham-operated eyes was achieved by P100–120, at which time *a*-waves were reliably recorded in five of the 11 transplanted eyes. No *a*-waves were recorded in age-matched sham-operated eyes.

STR-like responses appeared later in experimental groups (around P120) than in untreated rats (around P80). They also persisted slightly longer (up to P220), than in untreated eyes (up to P180).

3.2. Visual field thresholds recorded across the superior colliculus

Fig. 5(a) illustrates the progressive elevation in visual thresholds with age in untreated dystrophic RCS rats. Threshold values represent the average of thresholds from up to 76 respective RFs encompassing the whole visual field. In order to quantify the area of visual field preservation, another way of presenting this data, is to designate a threshold cut-off, and to plot the area of the visual field having thresholds under this cutoff, at various ages. Fig. 5(b) shows in unoperated dystrophic rats the progressive reduction with age of visual field area

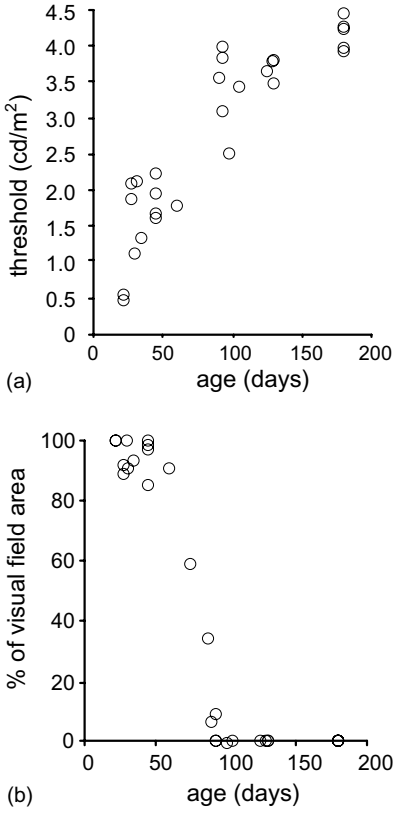

Fig. 5. Threshold responses recorded across the superior colliculus: (a) progressive elevation of threshold with age in untreated dystrophic RCS rats; threshold is presented as averages of individual RF thresholds; (b) progressive reduction of visual field area having thresholds lesser than 2.5 log cd/m^2 over low mesopic background (0.02 cd/m^2).

containing RFs with thresholds under 2.5 log cd/m^2 above background.

Subretinal transplantation led to a significant preservation of visual field area. Sham injections also resulted in lower thresholds than in untreated RCS rats: however, the area of rescue was more localized than following transplantation, being confined to the region of the trans-scleral injection site. The different outcome of transplant versus sham operation is illustrated in Fig. 6, which shows examples of threshold maps recorded across the whole SC, at 6 months of ages in all four animal groups studied: (a) non-dystrophics, (b) untreated dystrophics, (c) sham-operated dystrophics, and (d) transplanted dystrophics. These differences in the area of visual field preservation are expressed quantitatively in Fig. 7, which shows the percentage of visual field with RFs having thresholds at progressively higher cutoff levels. This histogram represents data from threshold maps recorded at 6 months of age in both experimental groups (sham and transplant operated, $n = 6$ respectively). Starting from 4.5 log, the lower the cutoff the more significant was the difference between the two groups: however, this difference became

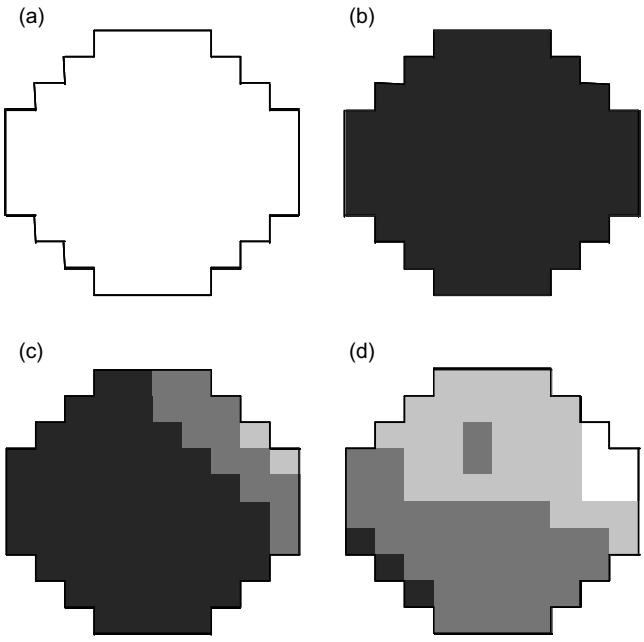

Fig. 6. Examples of maps at 6 months time point for (a) non-dystrophic, (b) untreated dystrophics, (c) sham-injected, and (d) transplant-injected eyes. Top and right respectively correspond to the retinotopic representation of the dorsal and temporal retina. Legend: white < 1; pale gray = 1–1.9; dark gray = 2–2.9; and black = 3–4.5 log cd/m^2 elevation in threshold above background.

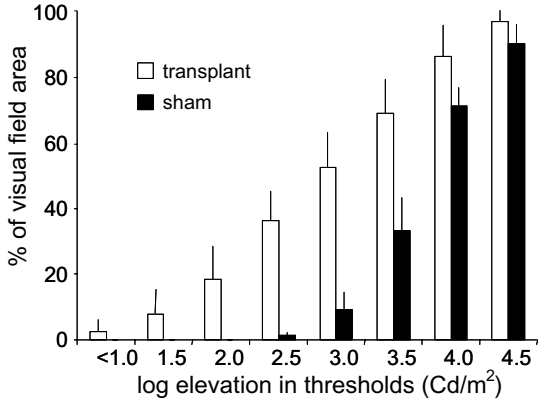

Fig. 7. Relative preservation of lower thresholds in transplant versus sham-operated eyes. The *Y*-axis represents the percentage of receptive fields (over total visual field area) having thresholds under the cut-offs indicated on the *X*-axis. Age 5 months, $n = 6$, error bars represent SEM.

non-significant at cutoffs lower than 2.0 log because too few points were recorded with such low threshold elevations (window of significance: between 2.0 and 3.5 log cutoffs, with highest significance at 3.0 log).

3.3. Correlation between ERG and visual field thresholds

Fig. 8 shows the relationship between the area of visual field preservation at various visual threshold cutoffs

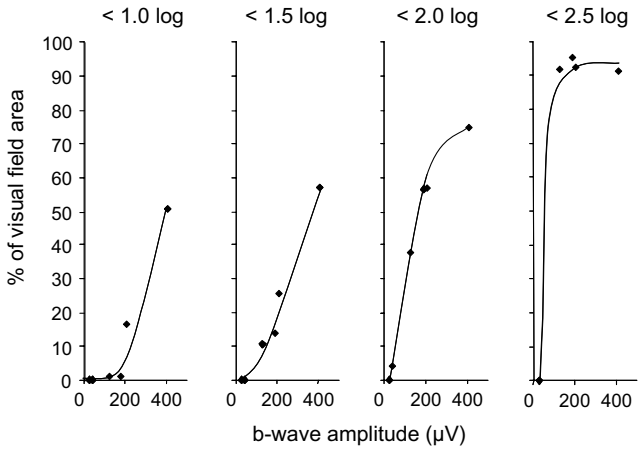

Fig. 8. Correlation between area of visual field preservation and maximum *b*-wave amplitude in untreated dystrophic RCS rats. Four different cut-offs are shown: 1.0, 1.5, 2.0 and 2.5 log elevation in visual thresholds.

and the corresponding *b*-wave amplitude in untreated dystrophic RCS rats. These graphs reflect data from animals aged between 28 days up to P100–120, i.e. the maximum time points at which *b*-waves can still be elicited in dark-adapted untreated RCS rats. Relationships approximating a linear fit were obtained using cutoffs of 1.5 and 2.0 log units. Most of the data underlying this linear relationship consisted of *b*-waves higher than 100 μV, which came from animals of up to P51 of age (see Fig. 1). Use of higher cutoffs gave plateaux. For instance, *b*-waves higher than 100 μV corresponded to a state in which most points across the visual field had thresholds under 2.5 log unit elevation.

It should be noted that in the case of animals with transplants or sham injections, the earliest visual field thresholds mapping was done at P150. In all cases, the *b*-wave maximal amplitudes were always under 100 μV. Between P150 and P180 of age, the corresponding *b*-wave amplitudes fitted best with visual field area having

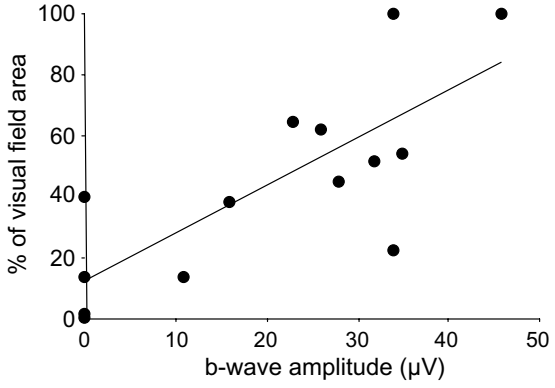

Fig. 9. Correlation between area of visual field preservation and maximum *b*-wave amplitude following transplant injection to dystrophic RCS rat eyes. Note the weaker correlation as compared with data from untreated dystrophic RCS rats. The best correlation was obtained using 3.0 log elevation as cut-off, $r^2 = 0.601$.

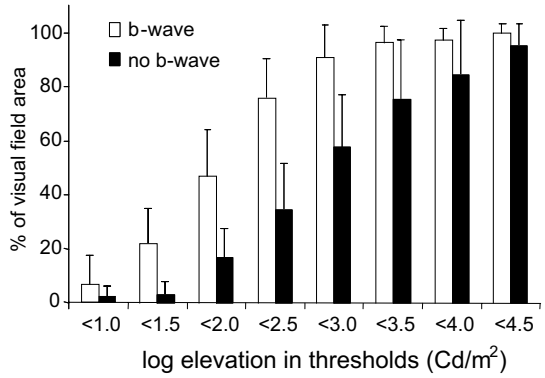

Fig. 10. ERG *b*-wave as a predictor of the extent of the area of visual field preservation after transplantation (recorded at 6–7 months of age). Eyes for which *b*-waves could be recorded (white bins) are associated with more extensive visual field preservation than in eyes with no *b*-wave response (black bins). Extent of visual field preservation (% of area) in function of visual thresholds. Cut-off of 2.5 log leads to the most significant discrimination between *b*-wave responsiveness or not.

thresholds under 3.0 log elevation ($r = 0.775$, $p = 0.0011$, Fig. 9).

Between P180 and P220, *b*-wave amplitudes tended to be under 50 μV. Since the criterion amplitude was 20 μV, this limited the operational range for variance to 30 μV and as a result, no correlation could be recorded between *b*-wave amplitude and area of visual field preservation. However, those retinae in which a *b*-wave could be recorded had more extensive visual field preservation than retinae without *b*-waves (Fig. 10). Significant differences between groups with and without *b*-waves were seen using threshold cutoff from 1.5 up to 3.5 log unit threshold elevation; optimal difference was obtained at 2.5 log units ($p = 0.0023$).

4. Discussion

4.1. Summary of the results

The results show that ERG *b*-wave responses elicited by full field stimulation provide a reliable indicator of the level of retinal function in RCS rats both during normal deterioration and after rescue by transplants. The size of the *b*-wave correlates with threshold levels and area of visual field rescue recorded from the SC. However, ERG responses, recorded under the present conditions, can be elicited only within a limited sensitivity range and they are ineffective in detecting activity associated with higher threshold responses. This is in accord with clinical studies where vision may still be present but an ERG response is no longer recordable (Sieving, 1999). In transplant studies, our results would suggest that a small area with preserved low visual RF thresholds, even though serving as a substrate for effective vision, might nevertheless be undetectable with standard full field ERG records. This would explain some of the ambiguity associated with previous reports of photoreceptor rescue with transplantation, which resulted in uncertain or negative corneal ERG responses to full field stimulation (Jiang & Hamasaki, 1994; Yamamoto, Du, Gouras, & Kjeldbye, 1993). Providing a correlation with another measure of visual function validates the value of full field ERG for screening the efficacy of transplantation, and defines its limitations in predicting the degree of central visual responsiveness.

In non-dystrophic rats, ERG and threshold records do not change significantly over the time frame studied (P21–180). In untreated dystrophic rats, the ERG *a*-wave disappears by 51 days and the *b*-wave between 80 and 100 days of age, preceding by several months the loss of visual responsiveness recorded in the superior colliculus, which occurs by around 180 days of age. This suggests that the two measures have different thresholds. When exploring whether any parameter of the ERG might show a relationship with threshold measures, the best correlation is found with *b*-wave amplitude. The maximal *b*-wave amplitude correlates with the area of visual field in which thresholds are less than 2.5 log elevation over background; this correlation holds only for data collected from animals of up to 100 days of age, since *b*-waves are no longer reliably recorded after. Preventive transplantation is effective in prolonging both ERG *b*-wave and visual RF responsiveness. ERG *b*-waves can be elicited up to 180 days of age and RFs mapped over part of the visual field up to 220 days of age. Including data from P150 to P180, the optimal relationship is obtained using 3.0 log elevation as the cut-off for RF area; however, the correlation between ERG and perimetry-like parameters is weaker than in untreated dystrophic rats.

4.2. ERG responses

Quantitative correlation is best achieved using *b*-wave amplitudes, although other components of the ERG response are affected by the progressive degeneration and by preventive transplantation. Interpretation of these changes depends on analysis of each component of the ERG waveform. As described previously (Bush et al., 1995), there is rapid loss of the *a*-wave over the first 50 days of life, which precedes the anatomical loss of rods (LaVail, Sidman, Rausin, & Sidman, 1974). While this may reflect loss of rod responses, there is some evidence for a small cone contribution to the *a*-wave in rodents (Lyubarsky et al., 2002; Nixon, Bui, Armitage, & Vingrys, 2001). This clearly is significant in the present work where we find preservation of *a*-wave responsiveness after transplantation up to as much as 3 months of age. Does this reflect continued rod activity or a small cone response? Results obtained in untreated dystrophic RCS rats indicate an early loss in rhodopsin

regeneration capability and light adaptation studies point to elevated threshold responses to a test spot even at 23 days of age (Perlman, 1978); both would suggest early compromise of rod function. Light adaptation curves after transplantation (Girman SV, ARVO Abstract #482, 2003) give no indication of preservation of low threshold responses (for backgrounds at least 2 log lower than used for tectal mapping here) suggesting that despite anatomical rescue of rods in such retinae, rod function may still be compromised. The remaining *b*-wave is presumed to be largely if not uniquely cone related and this contention is supported by ongoing work (Y. Sauvé et al., unpublished observations) using an adapting flash to bleach the retina prior to the test flash. While direct analysis of anatomical rescue and threshold responses have not been made in this study, previous work has shown that the density of cells in the outer nuclear layer (ONL) should be in the order of 70 cells/700 μm (equivalent to approximately 2 cells thickness in the ONL) for 2 log elevation in thresholds (Sauvé et al., 2002). Many of such ONL cells have the anatomical features of rods and the incidence of cones in rat retinae, of around 0.85% (Szel & Rohlich, 1992) is too low to account for these surviving cells. It appears therefore that remaining rods might be dysfunctional.

Among other ERG components affected by the progressive degeneration and preventive transplantation are the negative-going PIII and STR. In intact rats, PIII threshold is approximately 3 log units higher than that of the STR (Bush et al., 1995). The PIII component can also be elicited under higher background illumination than the STR, such as under photopic conditions. Therefore, PIII and STR can be reliably differentiated from each other based on the above-mentioned differences. A negative wave referred to as PIII has been used in a previous study (Jiang & Hamasaki, 1994) as a quantitative assessment of transplant-mediated retinal rescue in RCS rats. However, following retinal degeneration, due to uneven variations in thresholds from various ERG components, distinction between these components can only be reliably achieved through pharmacological intervention (Bush et al., 1995; Naarendorp, Sato, Cajdric, & Hubbard, 2001).

In the absence of background illumination, the STR is seen as a slow negative potential with the lowest visual thresholds of all ERG components (Frishman & Sieving, 1995). Based on pharmacological manipulations, the STR has been associated with activity from cells located in the proximal retina such as retinal ganglion cells and amacrine cells (Naarendorp et al., 2001). Using similar pharmacological approaches, Bush et al. (1995) have shown that the STR persists in aged RCS rats, at a time when no other components can be elicited. Our results support these findings: STR-like responses were the last ERG events preserved, regardless of the experimental group. The STR has been used as an indicator of visual function (Vollrath et al., 2001): however, in our hands, preservation of a waveform analogous to this component alone (at ages when the *b*-wave had vanished) does not correlate with the level of visual field preservation. A possibility, although purely speculative, could be that the STR-like wave in aged RCS might reflect phototransduction intrinsic to retinal ganglion cells (Berson, Dunn, & Takao, 2002; Hattar, Liao, Takao, Berson, & Yau, 2002), which could be modulated by loss of normal photoreceptor input.

4.3. Threshold responses

A comprehensive study of visual thresholds in RCS rats has been published elsewhere (Sauvé et al., 2001, 2002). In these as well as the present studies, the relative threshold responses were measured over backgrounds of 0.02 log cd/m^2. The time needed for dark adaptation would have made it impractical to measure absolute thresholds and furthermore, it has been pointed out in comparable studies using the Humphrey Field Analyzer in humans with RP (Jacobson et al., 1986) that it is crucial to test sensitivity under conditions that are pertinent to the subject's normal environment. The previous work validates the applicability of the approach in defining transplant-mediated rescue. Moreover, using this approach, a relationship was found between cell density of the ONL and threshold levels (Sauvé et al., 2002).

In the present study, this correlation has been taken a step further, showing that under specific conditions, there is also a relation between visual RF thresholds and ERG *b*-wave amplitude. The correlation comes at particular threshold levels. Such correlations have been explored clinically with widely variant results (Arden et al., 1983; Birch et al., 1987; Fahle et al., 1991; Iannaccone et al., 1995; Massof et al., 1984; Sandberg et al., 1996; Yagasaki et al., 1988). Best fits have been obtained when a single mutation is responsible for the deterioration in vision (Sandberg et al., 1996). Since the RCS dystrophic used here is highly inbred, that condition is met. One point of concern is that even when protected by transplantation, both ERG and visual thresholds show progressive deterioration. This may reflect the fact that xenografts were used and that the immunosuppressive regimen may not have been completely effective. From previous studies, in which animals were treated identically, an average blood level of cyclosporine of 250–300 μg/l of blood was maintained. However, it remains possible that there could be local fluctuations in cyclosporine levels, or that cyclosporine might not be the ideal immunosuppressive agent.

4.4. Correlation of ERG and perimetry results

In the case of transplants, the earliest visual field thresholds mapping was done at P150. Correlations

were obtained at P150–180 of age, when preserved *b*-waves had amplitudes under 100 μV. In comparison with correlation curves from untreated dystrophics (with maps available from a range of ages, the earliest being P28, and with *b*-waves of up to 400 μV), this places the data at the steepest part of the slope, where minor changes in *b*-wave amplitudes lead to high variations in the visual field area (see Fig. 8, using 2.5 log threshold cutoff). Despite the low amplitudes and smaller range of *b*-waves in the older rats, the Pearson correlation was $r = 0.775$, so $r^2 = 0.601$ which signifies that 60% of visual field area variation (under 3.0 log unit threshold elevation, as optimal cutoff) is accounted for by variation in the *b*-wave amplitude, while the remaining 40% is of unknown factors. While limiting the range of ERG amplitudes available has been shown to result in lower correlations (Sandberg et al., 1996), analysis of low *b*-wave amplitudes (1–10 μV), obtained using computer averaging of multiple traces can still reveal significant correlations with the area of visual field preservation in RP patients (Hood, Shady, & Birch, 1994).

In our study, *b*-waves were quantified from single traces using criterion amplitudes of 20 μV. While this is a high figure compared with some studies, lower thresholds were only achieved when larger numbers of recordings were averaged. This was not achieved to obviate complications due to response fragility that can be seen particularly during degeneration. Under the conditions of or recording, detectable *b*-waves vanished well before the lost of visual field responsiveness. Their occurrence required a minimal area of visual field depending on the threshold cutoff. For instance, for cutoffs of 3.0, 2.5 and 2.0 log units, the respective minimal area had to cover about 50%, 30%, and 15% of the visual field. Maintenance of low-thresholds in a minute area of the visual field (typical in >P150 shams) was not associated with detectable *b*-waves. For example, considering a sham-operated retina at P180 with 10% of the visual field under 2.0 log, no *b*-wave could be recorded in such case, despite obvious rescue effect.

5. Conclusion

The results show that measuring the amplitude of the *b*-wave provides a good indicator, albeit with limited sensitivity, of the progress of retinal disease and the efficacy of transplantation.

Acknowledgements

The work was supported by grants from Foundation Fighting Blindness, NIH (EY14038), Wynn Foundation, Research to Prevent Blindness and a joint equipment grant from the University of Utah. The authors would like to thank Drs. Sergej Girman, Shaomei Wang and Isabel Pinilla for their several contributions to this project.

References

Arden, G. B., Carter, R. M., Hogg, C. R., Powell, D. J., Ernst, W. J., Clover, G. M., Lyness, A. L., & Quinlan, M. P. (1983). Rod and cone activity in patients with dominantly inherited retinitis pigmentosa: comparisons between psychophysical and electroretinographic measurements. *British Journal of Ophthalmology, 67*, 405–418.

Berson, D. M., Dunn, F. A., & Takao, M. (2002). Phototransduction by retinal ganglion cells that set the circadian clock. *Science, 295*, 1070–1073.

Birch, D. G., Herman, W. K., deFaller, J. M., Disbrow, D. T., & Birch, E. E. (1987). The relationship between rod perimetric thresholds and full-field rod ERGs in retinitis pigmentosa. *Investigative Ophthalmology and Visual Science, 28*, 954–965.

Bourne, M. C., Campbell, D. A., & Tansley, K. (1938). Hereditary degenerations of the rat retina. *British Journal of Ophthalmology, 22*, 613–623.

Bush, R. A., Hawks, K. W., & Sieving, P. A. (1995). Preservation of inner retinal responses in the aged Royal College of Surgeons rat; evidence against glutamate toxicity in photoreceptor degeneration. *Investigative Ophthalmology and Visual Science, 36*, 2054–2062.

Chader, G. J. (2002). Animal models in research on retinal degenerations: past progress and future hope. *Vision Research, 42*, 393–399.

Coffey, P. J., Girman, S., Wang, S. M., Hetherington, L., Keegan, D. J., Adamson, P., Greenwood, J., & Lund, R. D. (2002). Long-term preservation of cortically dependent visual function in RCS rats by transplantation. *Nature Neuroscience, 5*, 53–56.

D'Cruz, P. M., Yasumura, D., Weir, J., Matthes, M. T., Abderrahim, H., LaVail, M. M., & Vollrath, D. (2000). Mutation of the receptor tyrosine kinase gene Mertk in the retinal dystrophic RCS rat. *Human and Molecular Genetics, 9*, 645–651.

Dowling, J. E., & Sidman, R. L. (1962). Inherited retinal dystrophy in the rat. *Journal of Cell Biology, 14*, 73–109.

Eisenfeld, A. J., LaVail, M. M., & LaVail, J. H. (1984). Assessment of possible transneuronal changes in the retina of rats with inherited retinal dystrophy: cell size, number, synapses, and axonal transport by retinal ganglion cells. *Journal of Comparative Neurology, 223*, 22–34.

Fahle, M., Steuhl, K. P., & Aulhorn, E. (1991). Correlations between electroretinography, morphology and function in retinitis pigmentosa. *Graefes Archives of Clinical and Experimental Ophthalmology, 229*, 37–49.

Frishman, L. J., & Sieving, P. A. (1995). Evidence for two sites of adaptation affecting the dark-adapted ERG of cats and primates. *Vision Research, 35*, 435–442.

Hattar, S., Liao, H. W., Takao, M., Berson, D. M., & Yau, K. W. (2002). Melanopsin-containing retinal ganglion cells: architecture, projections, and intrinsic photosensitivity. *Science, 295*, 1065–1070.

Hood, D. C., Shady, S., & Birch, D. G. (1994). Understanding changes in the *b*-wave of the ERG caused by heterogeneous receptor damage. *Investigative Ophthalmology and Visual Science, 35*, 2477–2488.

Iannaccone, A., Rispoli, E., Vingolo, E. M., Onori, P., Steindl, K., Rispoli, D., & Pannarale, M. R. (1995). Correlation between Goldmann perimetry and maximal electroretinogram response in retinitis pigmentosa. *Documenta Ophthalmologica, 90*, 129–142.

Jacobson, S. G., Voigt, W. J., Parel, J. M., Apathy, P. P., Nghiem-Phu, L., Myers, S. W., & Patella, V. M. (1986). Automated light- and dark-adapted perimetry for evaluating retinitis pigmentosa. *Ophthalmology, 93*, 1604–1611.

Jiang, L. Q., & Hamasaki, D. (1994). Corneal electroretinographic function rescued by normal retinal pigment epithelial grafts in retinal degenerative Royal College of Surgeons rats. *Investigative Ophthalmology and Visual Science, 35*, 4300–4309.

la Cour, M., Kiilgaard, J. F., & Nissen, M. H. (2002). Age-related macular degeneration: epidemiology and optimal treatment. *Drugs and Aging, 19*, 101–133.

LaVail, M. M., Sidman, M., Rausin, R., & Sidman, R. L. (1974). Discrimination of light intensity by rats with inherited retinal degeneration: a behavioral and cytological study. *Vision Research, 14*, 693–702.

Lund, R. D., Adamson, P., Sauvé, Y., Keegan, D. J., Girman, S. V., Wang, S., Winton, H., Kanuga, N., Kwan, A. S., Beauchene, L., Zerbib, A., Hetherington, L., Couraud, P. O., Coffey, P., & Greenwood, J. (2001a). Subretinal transplantation of genetically modified human cell lines attenuates loss of visual function in dystrophic rats. *Proceedings of the National Academy of Sciences USA, 98*, 9942–9947.

Lund, R. D., Kwan, A. S., Keegan, D. J., Sauvé, Y., Coffey, P. J., & Lawrence, J. M. (2001b). Cell transplantation as a treatment for retinal disease. *Progress in Retina and Eye Research, 20*, 415–449.

Lyubarsky, A. L., Lem, J., Chen, J., Falsini, B., Iannaccone, A., & Pugh, E. N., Jr. (2002). Functionally rodless mice: transgenic models for the investigation of cone function in retinal disease and therapy. *Vision Research, 42*, 401–415.

Machida, S., Chaudhry, P., Shinohara, T., Singh, D. P., Reddy, V. N., Chylack, L. T., Jr., Sieving, P. A., & Bush, R. A. (2001). Lens epithelium-derived growth factor promotes photoreceptor survival in light-damaged and RCS rats. *Investigative Ophthalmology and Visual Science, 42*, 1087–1095.

Massof, R. W., Wu, L., Finkelstein, D., Perry, C., Starr, S. J., & Johnson, M. A. (1984). Properties of electroretinographic intensity-response functions in retinitis pigmentosa. *Documenta Ophthalmologica, 57*, 279–296.

Naarendorp, F., Sato, Y., Cajdric, A., & Hubbard, N. P. (2001). Absolute and relative sensitivity of the scotopic system of rat: electroretinography and behavior. *Visual Neuroscience, 18*, 641–656.

Nixon, P. J., Bui, B. V., Armitage, J. A., & Vingrys, A. J. (2001). The contribution of cone responses to rat electroretinograms. *Clinical and Experimental Ophthalmology, 29*, 193–196.

Nusinowitz, S., Ridder, W. H., & Heckenlively, J. R. (2002). Electrodiagnostic techniques for visual function testing in mice. In R. Smith, S. W. M. John, P. M. Nishina, & J. P. Sundberg (Eds.), *Systematic evaluation of the mouse eye: anatomy, pathology, and biomethods*. New York: CRC Press.

Perlman, I. (1978). Dark-adaptation in abnormal (RCS) rats studied electrophysiologically. *Journal of Physiology London, 278*, 161–175.

Rivolta, C., Sharon, D., DeAngelis, M. M., & Dryja, T. P. (2002). Retinitis pigmentosa and allied diseases: numerous diseases, genes, and inheritance patterns. *Human and Molecular Genetics, 11*, 1219–1227.

Sandberg, M. A., Weigel-DiFranco, C., Rosner, B., & Berson, E. L. (1996). The relationship between visual field size and electroretinogram amplitude in retinitis pigmentosa. *Investigative Ophthalmology and Visual Sciences, 37*, 1693–1698.

Sauvé, Y., Girman, S. V., Wang, S., Lawrence, J. M., & Lund, R. D. (2001). Progressive visual sensitivity loss in the Royal College of Surgeons rat: perimetric study in the superior colliculus. *Neuroscience, 103*, 51–63.

Sauvé, Y., Girman, S. V., Wang, S., Keegan, D. J., & Lund, R. D. (2002). Preservation of visual responsiveness in the superior colliculus of RCS rats after retinal pigment epithelium cell transplantation. *Neuroscience, 114*, 389–401.

Sieving, P. (1999). Retinitis pigmentosa and related disorders. In M. Yanoff, & J. S. Duker (Eds.), *Ophthalmology, Section 8, Chapter 11* (pp. 1–10). St Louis: Mosby.

Szel, A., & Rohlich, P. (1992). Two cone types of rat retina detected by anti-visual pigment antibodies. *Experimental Eye Research, 55*, 47–52.

Vollrath, D., Feng, W., Duncan, J. L., Yasumura, D., D'Cruz, P. M., Chappelow, A., Matthes, M. T., Kay, M. A., & LaVail, M. M. (2001). Correction of the retinal dystrophy phenotype of the RCS rat by viral gene transfer of Mertk. *Proceedings of the National Academy of Sciences USA, 98*, 12584–12589.

Yagasaki, K., Jacobson, S. G., Apathy, P. P., & Knighton, R. W. (1988). Rod and cone psychophysics and electroretinography: methods for comparison in retinal degenerations. *Documenta Ophthalmologica, 69*, 119–130.

Yamamoto, S., Du, J., Gouras, P., & Kjeldbye, H. (1993). Retinal pigment epithelial transplants and retinal function in RCS rats. *Investigative Ophthalmology and Visual Science, 34*, 3068–3075.

Yamazaki, H., Ohguro, H., Maeda, T., Maruyama, I., Takano, Y., Metoki, T., Nakazawa, M., Sawada, H., & Dezawa, M. (2002). Preservation of retinal morphology and functions in Royal College Surgeons rat by nilvadipine, a Ca(2+) antagonist. *Investigative Ophthalmology and Visual Sciences, 43*, 919–926.